Malaysian Simulation SOCIETY
APPLICATIONS OF MODELLING AND SIMULATION
http://amsjournal.ams-mss.org
eISSN 2600-8084
VOL 2, NO. 1, 2018, 8-16

# Pole Placement Control of a 2D Gantry Crane System with Varying Pole Locations

Nafisat Muhammad Bashir[1], Amir Abdullahi Bature[1*] and Auwalu Muhammad Abdullahi[2]

[1]Department of Electrical Engineering, Bayero University Kano, Nigeria.
[2]Department of Mechatronics Engineering, Bayero University Kano, Nigeria.

[*]Corresponding author: aabature.ele@buk.edu.ng

**Abstract:** A gantry crane is widely used in industries for transportation of heavy loads, but control of this system for a fast operation is challenging. This paper presents the application of pole placement controller for controlling a 2D gantry crane system to achieve minimum sway angle and accurate positioning of payload by varying poles location. A linearized model of the system is obtained, and a pole placement controller is designed with three poles located at different locations on the left-hand side of the s-plane. Simulation via MATLAB and Simulink was performed to investigate the performance of the pole placement controller. Simulation results have shown that when both the dominant and other poles are chosen to be complex poles, then a better performance of the system will be achieved.

Keywords: Gantry crane system; Pole placement controller; Simulation.

## 1. INTRODUCTION

Gantry crane system (GCS) is of great importance where heavy loads are to be transported from one point to another easily. Gantry cranes are commonly used in material handling system in factories, warehouse, shipping yards and nuclear facilities where heavy loads must be moved with extraordinary precision [1]. It has been supported by two or more legs. The trolley is designed on the top of GCS to move and bring heavy loads either left or right along the horizontal bridge rail of a crane until accomplish to the desired location [1]. For modelling purposes, the GCS is considered as a pendulum like system. Gantry cranes are big and heavy, and most of them are mobile they can move from one point to another and are usually used in warehouse and shipyard, and sometime inside a factory, therefore a reduced simple model is the most suitable for analysis. A two-dimension (2D) trolley crane system transport loads in two dimensions; can lift the load vertically and move it in horizontal direction [1]. The crane should move the load as fast as possible without having any excessive payload sway at the final position. However, most of the common gantry cranes result in a swing motion when payload is suddenly stopped after a fast motion [2]. One of the characteristics of these cranes is the flexible hoisting ropes used as a part of the structure for the reduction of system mass, which result in favorable features of high payload ratio, high motion speed and low power consumption [3]. Figure 1 show a schematic diagram of a gantry crane considered in this work. $m_1$, $m_2$, $l$, $x$, $\theta$, $T$ and $F$ are payload mass, trolley mass, cable length, horizontal position of trolley, swing or sway angle, torque and driving force respectively. Figure 2 shows a real-life diagram of the gantry crane system. The GCS has two dependent generalized coordinates namely trolley displacement, $x$ and payload oscillation, $\theta$. There are several ways and methods that can be used in order to model the GCS [4].

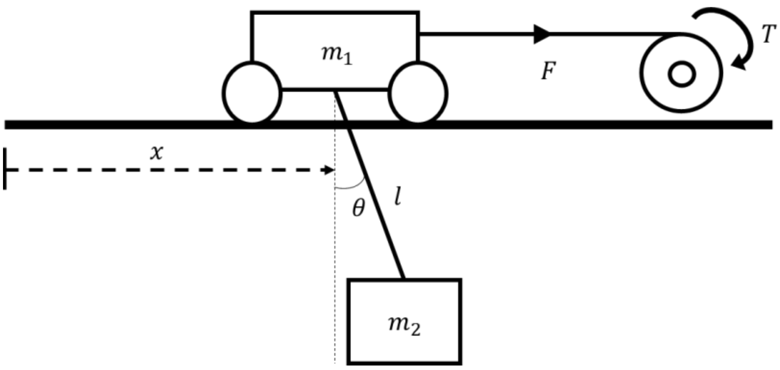


Figure 1. Schematic diagram of a nonlinear gantry crane system

Figure 2. Gantry crane system

To control GCS, many methods have been proposed to obtain good results. In [5], a model predictive controller is designed based on the linearized GCS and prediction cost function to ensure accurate positioning and oscillation reduction. In [6], the performance of Lyapunov pole placement (LPP), linear quadratic regulator (LQR) and proportional-integral-derivative (PID) control schemes for payload sway control and trolley position tracking of a gantry crane system were investigated. They used the response time specifications of the trolley position, level of payload sway reduction, and robustness to parameter variation and uncertainties to assess the performances of the controllers. In [7], a robust controller design procedure based on H∞ control theory to achieve fast trolley positioning with minimization of pendulum swinging was described. An optimal PID controller was used to control a nonlinear gantry crane system so as to move the trolley as fast as possible to the desired position with low payload oscillation technique in [8]. They employ Particle Swarm Optimization (PSO) in tuning the controller. In [9], linearized model of single pendulum gantry crane (SPGC) in state space form was used to design an output-delayed feedback controller (ODFC). The designed ODFC has undergone complete stability analysis for a given controller gain. In [10], the paper presents the design of controllers that will be able to transfer load from point to point as fast as possible with minimum load swing during the transfer process which vanishes at the load destination. These controllers were designed based on two approaches.

In the first approach, a gain-scheduling feedback controller was designed to move the load from point to point within one oscillation cycle without inducing large swings. In the second approach, the transfer process and the swing control are separated in the controller design. This approach requires designing two independent controllers: an anti-swing controller to reduce the load swing and a tracking controller for making the trolley follow a reference position trajectory. The objective of the first approach was achieved for small distances whereas for large distances, we have to decrease the gain which in turn slows the transfer process. In [11], three PID controllers for anti-swing, rope length and position control of a gantry crane were designed based on the parameters tuning method by particle swarm optimization (PSO). Satisfactory responses were obtained with the proposed controllers under conditions based on control system performances from simulation results. In [12], an electrical ducted fan design was proposed for active sway control of a gantry crane. The payload oscillation was cancelled by the thrust force developed by the motor. Satisfactory results were obtained from simulation results.

The main advantage of the approach is that it does not require modeling of the crane in real time experiments. Paper [5] presented the use of a model predictive controller to control a nonlinear 2D gantry crane system with a DC motor as an actuator. The controller was designed based on the linearized Gantry crane system and prediction cost function to ensure accurate positioning and oscillation. The closed-loop system was analyzed considering different cable length, payload mass and trolley position. It was found that the closed-loop control meets the main goal of this work, trolley positioning as fast as possible with minimum payload swinging all within a robust input voltage. In [13], a stable robust PID controller for anti-swing control of automatic gantry crane is proposed. The proposed method employs an automatic tuning using DE (differential evolution) to search for a set of PID controller gains that satisfy Kharitonov's polynomials robust stability criterion. This robust stability criterion is used to deal with parametric uncertainty occurs in gantry crane model. The simulation results show that a satisfactory robust PID control performance can be achieved. The PID controller is able to quickly move the cart of the crane while suppressing the swing of the payload for various conditions, i.e. payload mass and cable length variations.

Full State Feedback (FSF), or pole placement, is a method employed in feedback control system theory to place the closed-loop poles of a plant in pre-determined locations in the s-plane. Placing poles is desirable because the location of the poles corresponds directly to the eigenvalues of the system, which control the characteristics of the response of the system. The system must be considered controllable in order to implement this method. The pole placement controller works by placing poles at a desired position on the *s*-plane by giving priority to the dominant poles (poles closer to the imaginary axis). The location of the poles are specified by the designer, these locations can be on the real axis, imaginary axis or on both the two thus making the poles real, imaginary or complex poles respectively. The poles can either be on the left or right hand side of the *s*-plane which signifies stability or instability of the system respectively.

This paper presents a development of pole placement controller for GCS position control. Simulation is conducted within Matlab/Simulink environment to verify the performances of the controller by varying poles location. Trolley displacement and payload oscillation of the system are observed and analyzed. Simulation results have demonstrated satisfactory responses.

## 2. MODEL DERIVATION OF THE NONLINEAR 2D GANTRY CRANE

From [5] the nonlinear model equation of the crane can be summarized as follows;

$$F_x = (m_1 + m_2)\ddot{x}_1 + m_2 l\ddot{\theta}\cos\theta + m_2\ddot{l}\sin\theta + (2m_2\dot{l}\cos\theta - m_2 l\dot{\theta}\sin\theta)\dot{\theta} \tag{1}$$

$$l\ddot{\theta} + 2\dot{l}\dot{\theta} + \ddot{x}_1\cos\theta + g\sin\theta = 0 \tag{2}$$

The model equation is linearized as follows:
The motion equation are nonlinear due to the terms of sin $\theta$, cos $\theta$ and quadratic terms of them. According to the Taylor series expansion about operating point [5]:

$$F(x) = f(x_0) + (x - x_0)f'(x_0) + \frac{(x-x_0)^2}{2!}f''(x_0) + \frac{(x-x_0)^3}{3!}f'''(x_0) + \cdots + \frac{(x-x_0)^n}{n!}f^n(x_0) \tag{3}$$

$$\sin\theta = \sin\theta_0 + \cos\theta_0\,(\theta - \theta_0) \tag{4}$$

$$\theta_0 = 0 \text{ so } \sin\theta = \theta \tag{5}$$

$$\cos\theta = \cos\theta_0 - \sin\theta_0\,(\theta - \theta_0) \tag{6}$$

Hence,

$$\cos\theta = 1 \tag{7}$$

Because $\theta$ is assumed too small, $\dot{\theta}^2 = 0$, Equation (4) becomes Equation (5) and also Equation (6) becomes Equation (7) by putting $\theta_0 = 0$ . Since the tension force of hoisting rope is neglected so,

$$\ddot{l} = \dot{l} = 0 \tag{8}$$

Due to Equations (3), (5), (7) and (8), the nonlinear equations are linearized to Equations (8) and (9) which are expressed as follows:

$$F_x = (m_1 + m_2)\ddot{x}_1 + m_2 l\ddot{\theta} \tag{9}$$

$$l\ddot{\theta} + \ddot{x}_1 + g\theta = 0 \tag{10}$$

In terms of the *A*, *B*, *C*, *D* parameters that is in state space form, the linearized Equations (Equations (9) and (10)) of the gantry crane can be given as follows;

$$\dot{x} = Ax + Bu \tag{11}$$

$$y = Cx + Du \tag{12}$$

where $\dot{x}$ is the state vector, *y* is the system output, *A* is the system state matrix, *B* is the Input matrix, *C* is the output matrix and *D* is the transmission matrix.

$$A = \begin{bmatrix} 0 & 1 & 0 & 0 \\ 0 & 0 & \frac{m_2 g}{m_1} & 0 \\ 0 & 0 & 0 & 1 \\ 0 & 0 & \frac{-g(m_1+m_2)}{lm_1} & 0 \end{bmatrix} \quad B = \begin{bmatrix} 0 \\ \frac{1}{m_1} \\ 0 \\ \frac{-1}{lm_1} \end{bmatrix} \quad C = \begin{bmatrix} 1 & 0 & 0 & 0 \\ 0 & 0 & 0 & 0 \\ 0 & 0 & 1 & 0 \\ 0 & 0 & 0 & 0 \end{bmatrix} \quad D = \begin{bmatrix} 0 \\ 0 \\ 0 \\ 0 \end{bmatrix}$$

Table 1. Description of parameters

| Parameters | Value (unit) |
|---|---|
| Payload mass ($m_1$) | 0.5 kg |
| Trolley mass ($m_2$) | 2 kg |
| Cable length ($l$) | 0.5 m |
| Acceleration due to gravity ($g$) | 9.81 m/$s^2$ |

Table 1 shows the system parameters used in this work. Substituting the values of parameters in *A* and *B* yields;

$$A = \begin{bmatrix} 0 & 1 & 0 & 0 \\ 0 & 0 & 39.24 & 0 \\ 0 & 0 & 0 & 1 \\ 0 & 0 & -98.1 & 0 \end{bmatrix} \quad B = \begin{bmatrix} 0 \\ 2 \\ 0 \\ -4 \end{bmatrix} \quad C = \begin{bmatrix} 1 & 0 & 0 & 0 \\ 0 & 0 & 0 & 0 \\ 0 & 0 & 1 & 0 \\ 0 & 0 & 0 & 0 \end{bmatrix} \quad D = \begin{bmatrix} 0 \\ 0 \\ 0 \\ 0 \end{bmatrix}$$

## 3. CONTROLLER DESIGN

### 3.1 Pole Placement Controller Theory

Full state feedback (FSF), or pole placement, is a method employed in feedback control system theory to place the closed-loop poles of a plant in pre-determined locations in the s-plane. Placing poles is desirable because the location of the poles corresponds directly to the eigenvalues of the system, which control the characteristics of the response of the system. The system must be considered controllable to implement this method. This technique is widely used in systems with multiple inputs and multiple outputs, as in active suspension system. A system is said to be stable if the poles are located on the left-hand side of the s-plane or within the unit circle in the *z*-plane. The poles very close to the imaginary axis in s-plane or the poles closer to the right-hand side of the unit circle in the *z*-plane are called the dominant poles and they play a vital role in determining the stability of the system.

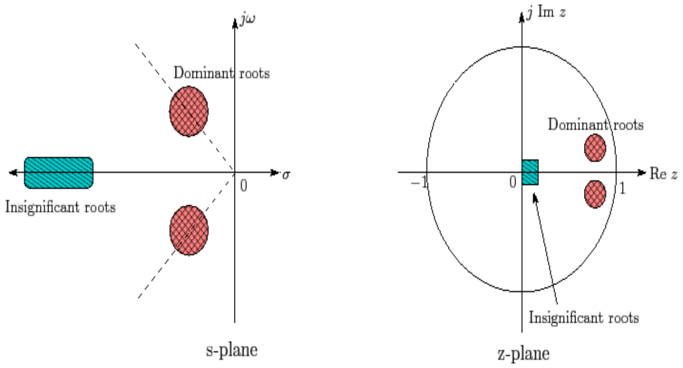


Figure 3. Position of poles on the s-plane and z-plane

### 3.2 Pole Placement Controller Design

The pole placement controller works by placing poles at a desired position on the s-plane by giving priority to the dominant poles (poles closer to the imaginary axis). The location of the poles is specified by the designer, these locations can be on the real axis, imaginary axis or on both the two thus making the poles real, imaginary or complex poles respectively. The poles can either be on the left or right-hand side of the s-plane which signifies stability or instability of the system respectively. In general, the second order transfer function can be written as,

$$G(s) = \frac{K{\omega_n}^2}{s^2 + 2\zeta\omega_n s + {\omega_n}^2} \tag{13}$$

Parameter *K* is a gain/constant. The poles of the general transfer function can be found from the denominator of closed-loop transfer function as,

$$s_{1,2} = -\zeta\omega_n \pm j\omega_n\sqrt{1-\zeta^2} \tag{14}$$

Now test the system response to the unit step input signal. Let us analyses the output response for various cases depend on the value of $\zeta$(damping ratio), which has a relationship with the poles location on s-plane. From Equation (13), using partial differential equation (PDE), if the test input signal is a unit step (1/s):

$$C(s) = \frac{1}{s} . \frac{{\omega_n}^2}{s^2 + 2\zeta\omega_n s + {\omega_n}^2} = \frac{K_1}{s} + \frac{K_2 s + K_3}{s^2 + 2\zeta\omega_n s + {\omega_n}^2} \tag{15}$$

Assume that $\zeta < 1$, for the case under-damped, obtain the value of $K_1$, $K_2$ and $K_3$. Next step is to obtain $c(t)$ by taking the inverse Laplace transform of $C(s)$,

$$c(t) = 1 - e^{\zeta\omega_n t}\left\{\cos\omega_n\sqrt{1-\zeta^2}t + \frac{\zeta}{\sqrt{1-\zeta^2}}\sin\omega_n\sqrt{1-\zeta^2}t\right\} \tag{16}$$

or

$$c(t) = 1 - \frac{1}{\sqrt{1-\zeta^2}}e^{\zeta\omega_n t}\cos\left(\omega_n\sqrt{1-\zeta^2}t - \varphi\right),\ \varphi = \tan^{-1}\frac{\zeta}{\sqrt{1-\zeta^2}} \tag{17}$$

a) Rise time, $T_r$:

Time required for waveform to go from 0.1 (10%) of final value to 0.9 (90%) of the final value.

$$T_r = \left|t_{0.9c(t_{final})} - t_{0.1c(t_{final})}\right| \tag{18}$$

b) Peak time, $T_p$:

Time required to reach the first maximum peak ($c_{max}$) of the waveform. From Equation (14), rearranging and completing the squares in the denominator to produce:

$$sC(s) = \frac{\omega_n}{(s+\zeta\omega_n)^2 + \omega_n(1-\zeta^2)}$$

$$\dot{c}(t) = \frac{\omega_n}{\sqrt{1-\zeta^2}}e^{\zeta\omega_n T_p}\sin(\omega_n\sqrt{1-\zeta^2}t) \tag{19}$$

Setting the derivative equal to zero yields,

$$\omega_n\sqrt{1-\zeta^2}t = n\pi; \quad t = \frac{n\pi}{\omega_n\sqrt{1-\zeta^2}} \tag{20}$$

Therefore, the first peak ($n$ = 1) is the maximum $c$, which is called peak time $T_p$:

$$T_p = \frac{\pi}{\omega_n\sqrt{1-\beth^2}} \tag{21}$$

c) Percentage overshoot, $\%OS$:

The amount that waveform overshoots from the steady-state or final value. $c_{max}$ is $c(T_p)$, can be calculated as:

$$\%OS = \frac{c(T_p) - c(t_{final})}{c(t_{final})} \times 100\% \quad \frac{c_{max} - c_{final}}{c_{final}} \times 100\% \tag{22}$$

$c_{max}$ can be obtained by evaluating $c(t)$ at $T_p$, from Equation (21). Substituting Equation (21) into Equation (16),

$$C_{max} = c(T_p) = 1 - e^{\frac{\zeta\pi}{\sqrt{1-\zeta^2}}}\cos\left(\pi + \frac{\zeta}{\sqrt{1-\zeta^2}}\sin\pi\right) = 1 + e^{\zeta\pi/\sqrt{1-\zeta^2}} \tag{23}$$

$c_{final} = 1$ (for this case)

finally find,

$$\%OS = e^{-\zeta\pi/\sqrt{1-\zeta^2}} \times 100\% \tag{24}$$

d) Settling time, $T_s$:

Time required for the transients damped oscillations to reach and stay within ±2% (or ±5%) of the steady-state value. For the case ±2%, if the final state is 1, the settling time can be calculated when the output $c(t)$ is within (0.98< $c(t)$ <1.02). From Equation (23),

$$c(T_s) = 1 - \frac{1}{\sqrt{1-\zeta^2}} e^{\zeta\omega_n T_s} \cos\left(\omega_n \sqrt{1-\zeta^2} T_s - \varphi\right) = 0.98 \quad (25)$$

therefore,

$$\frac{1}{\sqrt{1-\zeta^2}} e^{\zeta\omega_n T_s} \cos\left(\omega_n \sqrt{1-\zeta^2} T_s - \varphi\right) = 0.02$$

$$T_s = \frac{-\ln\left(0.02\sqrt{1-\zeta^2}\right)1}{\zeta\omega_n} \cong \frac{4}{\zeta\omega_n}$$

By choosing (a): Settling time, $T_s = 2$ secs and percentage overshoot, $OS$ = 0.1%, a stable pole location can be obtained at:

$$P_1 = [-2.0 + 0.5i \quad -2.0 - 0.5i \quad -30 \quad -40] \quad (26)$$

Also, choosing a settling time, $T_s$ = 2.66 secs and percentage overshoot, $OS$ = 0.05%, we obtained a stable pole location at:

$$P_2 = [-1.5 + 0.5i \quad -1.5 - 0.5i \quad -1.0 + 1.0i \quad -1.0 - 1.0i\,] \quad (27)$$

Also choosing a settling time, $T_s = 2$ secs and a percentage overshoot, $OS$ = 0.15%, we obtained a stable pole location at:

$$P_3 = [-2.0 + 1.0i \quad -2.0 - 1.0i \quad -1.0 + 3.0i \quad -1.0 - 3.0i] \quad (28)$$

The gain $K$ can be obtained using Matlab command, $K$= acker($A$, $B$, $p_k$ ). For the first case that is, choosing the dominant pole pairs to be complex poles and the other two poles to be real poles as in $P_1$, the pole placement controller had a gain of $K_1$= [129.9694 129.9057 -281.5528 46.4529]. For the second and third cases that is, choosing both the dominant and the other poles to be complex poles as in $P_2$ and $P_3$, the pole placement controller had gains of $K_2$= [0.1274 0.2803 21.9637 -1.1098] and $K_3$= [1.2742 1.2742 19.4121 -0.8629].

## 4. RESULTS AND DISCUSSION

### 4.1 Closed-Loop Response

The reference tracking was carried out using two different reference inputs to the simulation environment. The first input is a step signal and the second input is a pulse signal. Each simulation is carried out using the pole placement controller with different pole locations and the resulting output and control signals are shown in different plots.

To achieve a perfect tracking, different pole locations are tested to see which pole location gives the accurate reference tracking and which pole location gives the minimum sway angle. The location of poles plays a significant role in enhancing or deteriorating the performance of the system.

#### *4.1.1 Response due to Step Input*

When a step input is applied, the output position response, sway angle response and control signal are shown in Figures 4-6 respectively. From Figure 4, the different pole locations have different responses. At pole location $P_1$, the step input was tracked at a settling time of 2.84 secs. At pole location $P_2$, the step input was tracked at a settling time of 4.17 secs. At pole location $P_3$, the step input was tracked at a settling time of 2.39 secs.

From Figure 5, when the pole location is $P_1$, the sway angle deviates between -17° to 3.5° at the expense of fast tracking of step input before stabilizing at 0° after 3.5 secs. When the pole location is $P_2$, the sway angle deviates between -2.5° to 1° at the expense of zero overshoot while tracking the step input before stabilizing at 0° after 5.4 secs. When the pole location is $P_3$, the sway angle deviates between -10° to 8.5° at the expense fast tracking of step input before stabilizing at 0° after 5.4 secs.

From Figure 6, the different control signals due to the pole locations are shown. At pole location $P_1$ the pole placement controller requires 129.97 Nm control signal. At pole location $P_2$, the controller has a 0.89 Nm. At pole location $P_3$, the controller has a control signal of nearly 3.80 Nm. Figure 7 shows a clear view of the signals in Figure 6.

Conclusively, when the dominant poles pair are complex poles and the other poles are real poles (that is, pole location $P_1$), the system demanded a high torque. But when both the dominant and the other poles are complex poles, the system demanded a low torque. Summary of the response due to step input is shown in Table 2.

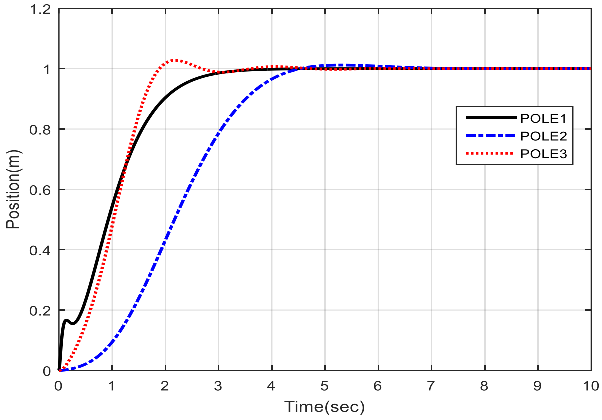


Figure 4. Position response of the closed-loop system due to step input

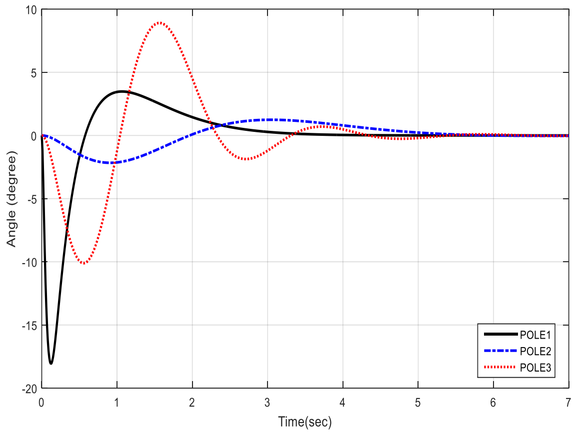


Figure 5. Sway angle response of the closed-loop system due to step input

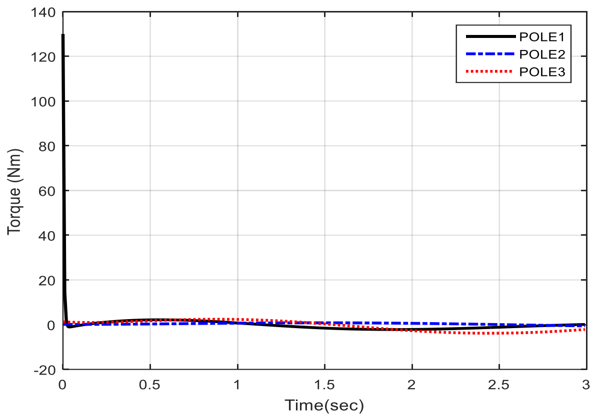


Figure 6. Control signal of the closed-loop system due to step input

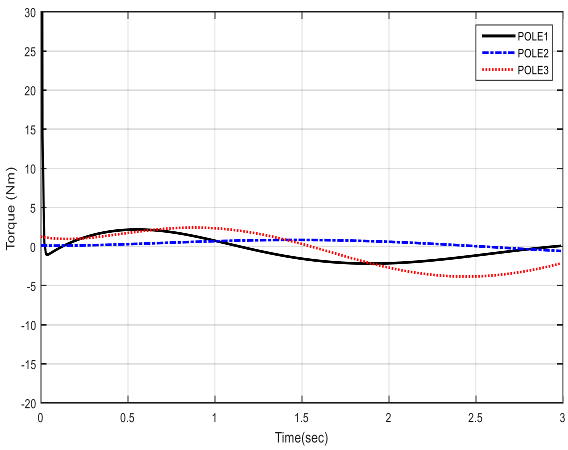


Figure 7. Control signal of the closed-loop system due to step input

Table 2. Summary of responses due to step

| Pole locations | Settling time (s) | Maximum sway angle (deg.) | Maximum control signal (Nm) | Overshoot (%) |
|---|---|---|---|---|
| Pole 1 | 2.84 | 17.00 | 129.97 | 0.00 |
| Pole 2 | 4.17 | 2.50 | 0.89 | 1.22 |
| Pole 3 | 2.39 | 10.00 | 3.80 | 2.77 |

*4.1.2 Response due to Pulse Input*

When a pulse input is applied, the output response and the control signal can be seen in Figures 8-11.

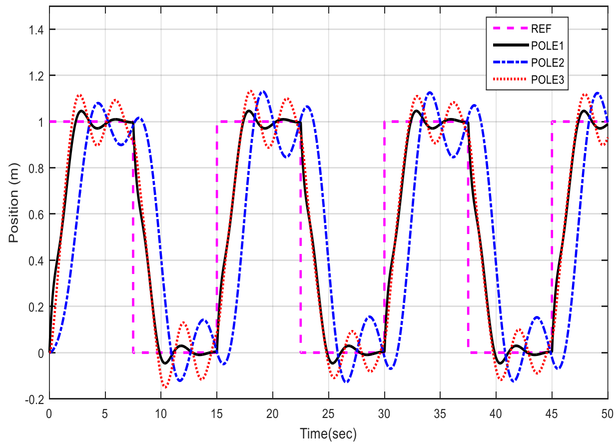


Figure 8. Position response of the closed-loop due to pulse input

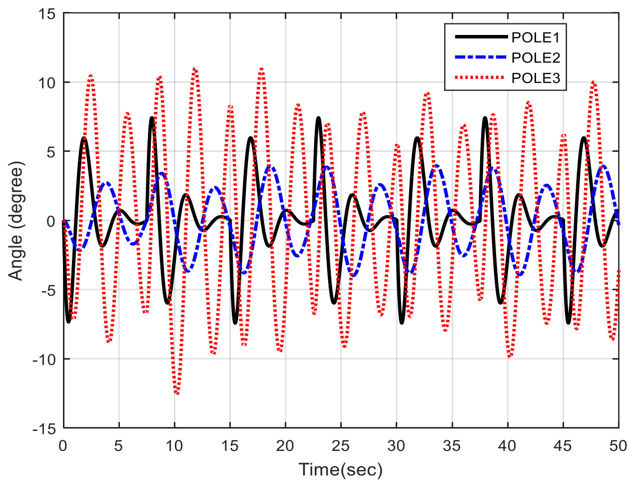


Figure 9. Sway angle response of the closed-loop system due to pulse input

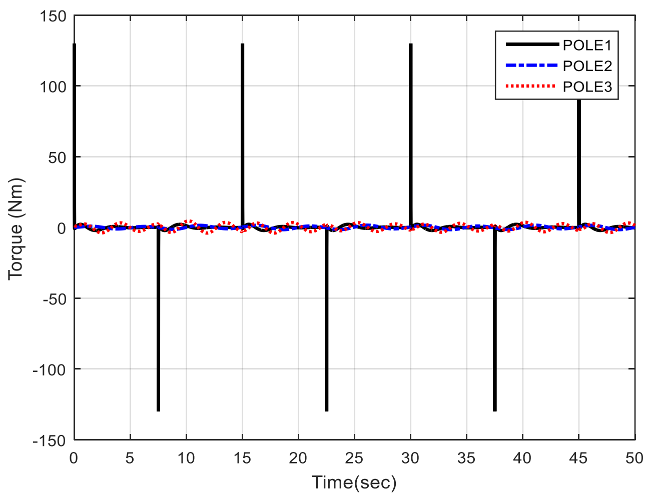


Figure 10. Control signal of the closed-loop system due to pulse input

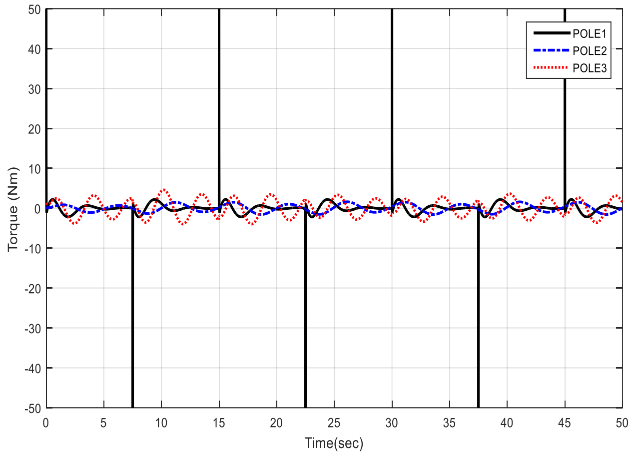


Figure 11. Control signal of the closed-loop system due to pulse input

From Figure 10, the different control signals due to the pole locations are shown. It can be seen that at pole location $P_1$ the system requires 130 Nm control signal. At pole location $P_2$ the system requires 2 Nm control signal. At pole location $P_3$, the system requires 5 Nm control signal. Figure 11 shows a clear view of Figure 10. Conclusively, it can be seen that when the dominant poles are complex poles and the insignificant poles are real poles (that is, pole location $P_1$), the controller demanded a high voltage control signal at specific time intervals. But when both the dominant and the insignificant poles are complex poles, the controller demanded a low voltage control signal at all period of time.

## 5. CONCLUSION

This paper has examined different pole locations of pole placement control for a 2D gantry crane. Based on the results obtained, it can be concluded that pole placement location $P_1$ where the dominant poles are complex poles and the other poles are real poles and are located far away from the imaginary axis contributed to a fast settling of the system with nearly zero overshoot but at the expense of the highest sway angle and made the system to consume a very large energy. Pole placement location $P_2$ where all the poles are complex poles and are located very close to the imaginary axis contributed to a delayed settling of the system with little overshoot but with very small sway angle with small energy consumption. Poles located at $P_3$ contributed to a better settling of the system more than $P_2$ but with a sway angle and overshoot which is more than that of $P_2$ at the expense of minimum energy consumption.

## REFERENCES


[1] M. J. Maghsoudi, Z. Mohamed A. F. Pratiwi, N. Ahmad and A.R. Husain, An experiment for position and sway control of a 3D gantry crane, *4th International Conference on Intelligent and Advanced Systems*, Malaysia, 2012 pp. 497–502.

[2] W. J. Jalani, R. Muhida and M. Jimoh and E. Salami, Control strategy for automatic Gantry crane systems: a practical and intelligent approach, *International Journal of Advanced Robotic Systems*, 4, 447–456, 2007.

[3] M. Azdiana Z. Mohamed and N. A. Sulaiman, Inverse Dynamic analysis with feedback control for vibration-free positioning of a gantry crane system, *International Conference on Electronic Design*, Penang, Malaysia, 2008, pp. 1–5.

[4] H. I. Jaafar, Z. Mohamed, J. J. Jamian, A. F. Abidin, A. M. Kassim and Z. Ab Ghani, Dynamic behavior of a nonlinear gantry crane system, *Procedia Technology*, 11, 419–425, 2013.

[5] N. K. Dankadai, A. Athif, M. Faudzi, A. Bature and M. I. Faruk, Position control of a 2D nonlinear gantry crane system using model predictive controller, *Applied mechanics and materials*, 735, 282–288, 2015.

[6] A. Alhassan, K. A. Danaplasingam, M. Shehu, A. M. Abdullahi and A. Shehu, Closed-loop schemes for position and sway control of a gantry crane system, *International Journal of Simulation: Systems, Science and Technology*, 17, 1–8, 2016.

[7] I. Burul, F. Kolonic, J. Matusko, The control system design of a gantry crane based on H-infinity control theory, *The 33rd International Convention MIPRO*, Opatija, Croatia, 2010, pp. 183–188.

[8] H. I. Jaafar, Z. Mohamed, A. F. Zainal Abidin and Z. Ab Ghani, PSO-tuned PID controller for a nonlinear gantry crane system, *IEEE International Conference on Control System, Computing and Engineering*, Malaysia, 2012, pp. 515–519.

[9] Rajeeb Dey, Nishant Sinha, Priyanka Chaubey, S. Ghosh and G. Ray, Active sway control of a single pendulum gantry crane using output-delayed feedback control technique, *11th International Conference on Control Automation, Robotics and Vision*, Singapore, 2010, pp. 532–536.

[10] H. Omar, *Control of gantry and tower cranes*, Ph.D. Dissertation, Virginia Polytech. Inst. and State Univ., Blacksburg, Virginia, 2003.

[11] D. V. Diep and V. V. Khoa, PID control tuning optimization with PSO algorithm for nonlinear gantry crane system, *International Journal of Engineering and Computer Science*, 3(6), 6631–6635, 2014.

[12] M. J. Maghsoudi and Z. Mohamed, Active sway control of a gantry crane by an electric ducted fan, *International Journal of Acoustics and Vibration*, 20, 171–176, 2015.

[13] M. I. Solihin, Robust PID controller tuning for 2D gantry crane using Kharitonov's theorem and differential evolution optimizer, *Advanced Materials Research*, 903, 267–273, 2014.